Evaluation of Basilar Artery Atherosclerotic Plaque Distribution by 3D High Resolution MR Vessel Wall Imaging and Semi-Automatic Analysis Tool

Zhensen Chen[1], Huijun Chen[1], Aofei Liu[2], Wei-Jian Jiang[2], William Kerwin[3], Chun Yuan[1,3], and Xihai Zhao[1]

[1]*Center for Biomedical Imaging Research & Department of Biomedical Engineering, Tsinghua University, Beijing, China,* [2]*New Era Stroke Care and Research Institute, The Second Artillery General Hospital PLA, Beijing, China,* [3]*Department of Radiology, University of Washington, Seattle, WA, United States*

Introduction: Disruption of vulnerable atherosclerotic plaque at basilar artery (BA) is the major cause of posterior circulation infarction. Angioplasty with or without stent is a treatment strategy for BA revascularization. However, stenting of BA stenosis has the highest risk of periprocedural complications, especially perforator strokes among stenting of intracranial arteries (intracranial carotid, middle cerebral, intracranial vertebral and basilar artery). Previous studies have shown that this may be due to the plaque is pushed during stenting and blocks the ostia of BA's perforating arteries which originate from the lateral or dorsal walls of BA[1,2]. Thus, characterizing BA plaque distribution is of great significance for preoperative evaluation of stenting procedure. Recent development of 3D MR vessel wall imaging techniques [3-6] might allow comprehensive assessment of plaque characteristics with higher accuracy by accounting for the nature curvature of artery. **This study sought to propose an analysis tool to semi-automatically evaluate the distribution of BA plaque based on 3D high resolution MR vessel wall images.**

Methods: After written informed consent obtained, 58 symptomatic patients with neurovascular diseases indicated by routine examinations underwent intracranial MR angiography and 3D high resolution black-blood vessel wall imaging at a 3.0T whole body scanner (Achieva TX, Philips, Best, Netherlands) with a custom-designed 36-channel neurovascular coil. The imaging parameters were as follows: (1) 3D TOF-MRA: FFE, TR/TE 25/3ms, FOV 200×200×84mm, matrix size 400×400×60. (2) 3D VISTA-PDW [5]: TSE, TR/TE 2000/32ms, FOV 160×160×45mm, matrix size 320×320×45. (3) 3D SNAP [6]: FFE, TR/TE 10/4.8ms, FOV 250×160×40mm, matrix size 312×200×50. ***Image processing:*** The flow chart for our proposed image processing tool is shown in **Fig.1**. **Of note, in step ⑤, the cross-sectional images were generated perpendicular to the centerline**; and the lumen and wall contours in cross-sectional slice were calculated by connecting 8 intersection points of the unclosed boundaries from step ④ and slice using closed spline curves, which allow manual adjustment. By using this analysis tool, the following measurements can be semi-automatically achieved: 1) Division of quadrants; 2) Vessel wall area and lumen area in each quadrant; 3) Wall thickness (WT) at 120 equiangular radial directions. ***Data analysis:*** For each plaque in BA, its location relative to AICA on VISTA and the presence of intraplaque hemorrhage (IPH) on SNAP were identified and the length was measured using Philips MR work station. With the proposed analysis tool, we can determine: 1) Normal BA wall thickness: this can be obtained from the cross-sectional slices that are free of plaque; 2) Automatic detection of BA plaques: When the maximum WT (maxWT) of a quadrant was larger than the normal WT plus 2 times of its standard deviation, the presence of plaque will be considered; 3) The quadrant with maxWT for each plaque; 4) Stenosis index (1-total lumen area of the slice with plaque / total lumen area of reference slice).

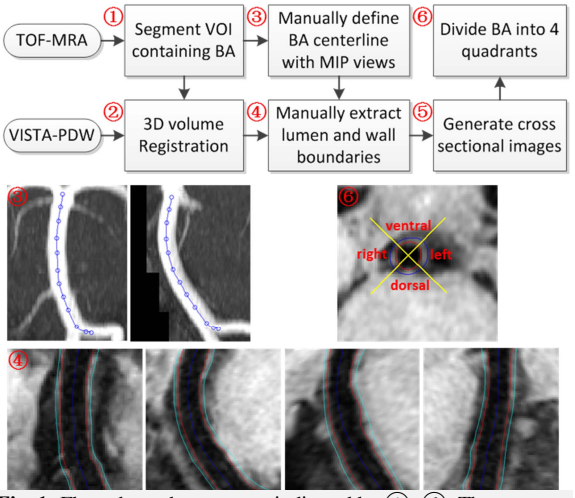

Fig. 1: Flow chart: the steps are indicated by ①~⑥. The corresponding images of step ③, ④ and ⑥ are also shown. VOI: volume of interest, MIP: maximum intensity projection.

Results: Of 58 subjects (41 males, mean age 55.7 years), 33 (56.9%) developed 43 plaques in BA, including 24 with 1 plaque, 8 with 2 plaques, and 1 with 3 plaques. The length and maximum stenosis index of plaques was 11.5±5.9mm and 40.7±31.5%, respectively. IPH was found in 18.6% (8/43) plaques. The percentage of BA plaques that affected each quadrant was detailed in **Fig. 2**. We found that 58.1% plaques affected wall in all four quadrants (**Fig. 3**) and 34.9% and 37.2% plaques mainly affected the ventral and right quadrant, respectively (**Fig. 4**). Of 43 BA plaques, 69.8% were found at the BA segment distal to AICA. **Fig.5** shows a typical vulnerable BA plaque with IPH.

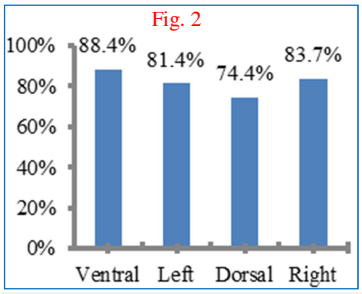

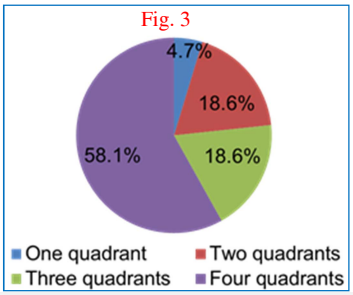

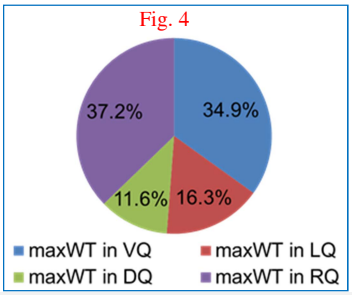

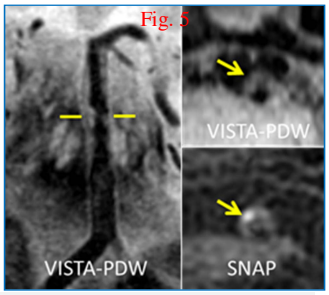

Fig. 2: Percentage of plaques affecting different quadrants; **Fig. 3:** Cross-sectional extent of plaques; **Fig. 4:** Distribution of plaque's maxWT. The VQ, LQ, DQ and RQ represent ventral, left, dorsal, and right quadrant, respectively. **Fig. 5:** A typical vulnerable BA plaque. IPH shows hyperintense on SNAP images.

Discussion and Conclusions: The developed semi-automatic analysis tool facilitates identification of vessel centerlines and lumen and wall contours, and allows comprehensive characterization of BA plaques, such as cross-sectional distribution, stenosis and burden measurements. The normal BA wall thickness we presented in this study is larger than that of previous studies [5]. This may be due to the different study population. The partial volume effect from the non-isotropic acquisition may also contribute to this result. **In this study, we found that most of the plaques in BA (95.3%) tended to affect multiple quadrants and more than 60% plaques mainly affected the areas of arterial wall where perforating arteries originate to feed pons, suggesting that it is necessary to assess the BA plaque distribution prior to stenting treatment.** In addition, our results indicates that the prevalence of multi-plaques in BA was high (27.3%) and the longitudinal extent of plaques was large (11.5±5.9mm). This does prompt demand for 3D MR plaque imaging with large coverage and imaging processing tools.

References: 1. Levy EI, et al. JNS. 2003;99(4):653-60; 2. Marinkovic SV, et al. Neurosurgery. 1993;33(1):80-7; 3. Balu N, et al. MRM. 2011;65(3):627-37; 4. Fan Z, et al. JMRI. 2010;31(3):645-54; 5. Qiao Y, et al. JMRI. 2011;34(1):22-30; 6. Wang J, et al. MRM. 2013;69(2):337-45